npj | climate and atmospheric science

Article

Published in partnership with CECCR at King Abdulaziz University

https://doi.org/10.1038/s41612-024-00842-8

Internal variability of the winter North Atlantic Oscillation longitudinal displacements

María Santolaria-Otín ✉ & Javier García-Serrano

The winter North Atlantic Oscillation (NAO), one of the leading modes of atmospheric variability in the Northern Hemisphere and key driver of surface climate anomalies, was long considered to be spatially stable. Yet, its northern center-of-action – the Icelandic Low (IL) – shifted eastward in the late 1970s compared to the preceding decades of the mid-20th century. The responsible processes are still uncertain, particularly after the decline of the positive NAO trend in the 21st century. Here, we present observational and model evidence that the NAO-IL moves naturally alternating between two preferential locations, west/east of Iceland, with no need for changes in anthropogenic forcing or low-frequency oceanic variability. These recurrent longitudinal displacements of the NAO pattern appear linked to zonal changes in the fluctuations (not mean-state) of transient-eddy activity, emphasizing the relevance of internal atmospheric variability, and could represent a major source of uncertainty in regional climate prediction and projection.

The North Atlantic Oscillation (NAO) is the dominant mode of atmospheric variability in the Euro-Atlantic sector, particularly during winter when it can explain up to 50% of the sea level pressure (SLP) variance. It is classically described as a meridional seesaw of SLP anomalies between the subpolar Icelandic Low (IL) and the subtropical Azores High (AH)[1,2]. In its positive phase, both centers-of-action are reinforced, and the westerly winds are intensified; the storm-track is displaced poleward bringing warmer air and more precipitation over north-western Europe, whereas relatively colder and drier conditions prevail over southern Europe. Variability of the latitudinal position and strength of the North Atlantic jet are reflected in the signature of the NAO pattern[3]; which is an eddy-driven atmospheric phenomenon maintained by synoptic activity[4,5], emerging prominently at a wide range of timescales, from daily to multi-decadal[6–9]. The NAO has a substantial impact on surface climate of the surrounding continents as well as on the occurrence of extreme weather events downstream[10,11]. Gaining insight into the nature of the NAO variability is essential to improve its predictability, and thus mitigate its potential impacts on water resources, public health and ecosystems[12–15].

Although the NAO is probably one of the most studied modes of climate variability, the understanding of its dynamics and spatio-temporal characteristics is still far from complete. It is quite common to discuss the NAO signal assuming that the spatial pattern of both centers-of-action remains steady. However, it has been shown that the IL and AH experience notable changes in their position through time[16–21]. Hilmer and Jung[16] first evidenced an eastward shift of the northern lobe (IL) by analysing the link between the winter NAO and Arctic sea-ice export through the Fram Strait. They found that its correlation was only significant during the period 1978−1997, as opposed to 1958−1977, when the northern center of the NAO moved eastward carrying anomalous northerly wind through the Fram Strait. Further, a coherent picture in variability coincident with the NAO eastward shift was found in other variables such as surface temperature over Europe and Siberia as well as in the storm-track over the North Atlantic Ocean and the Baltic Sea[22–24]. The zonal shift in the northern lobe of the NAO has also been proved to have an important effect on precipitation over Europe[25,26] and even remotely, over High Mountain Asia[27].

Different hypotheses have been proposed to explain the cause of the longitudinal displacements in the NAO pattern. On the one hand, it has been argued that the eastward shift may have been associated with increasing greenhouse gas (GHG) forcing and the related sea surface temperature (SST) warming[28,29], implying a possible link to anthropogenic climate change during the last decades of the 20th century. In line with this argument, Peterson et al.[30,31] proposed that the eastern (western) position of the IL was related to non-linear dynamics of a positive (negative) NAO phase, thereby the observed eastward shift reported by Hilmer and Jung[16] was a consequence of the observed trend towards a positive NAO index by the end of the 20th century. A similar hypothesis but analysing Rossby wave breaking and Greenland blocking was proposed by Wang and Magnusdottir[32] and Davini et al.[33], respectively. However, it is now accepted that the trend in the NAO index weakened and even reversed at the beginning of the 21st century, besides an enhanced GHG forcing and a

Group of Meteorology, Universitat de Barcelona, Barcelona, Spain. ✉e-mail: m.santolaria-otin@meteo.ub.edu

stronger global warming[34]; thus, apparently limiting the causal relationship between the phenomena.

On the other hand, Börgel et al.[35], using a multi-centennial paleoclimate simulation, have suggested that the zonal changes in the position of both NAO centers-of-action can be associated with internal oceanic low-frequency variability, namely the Atlantic Multidecadal Oscillation (AMO): during a positive phase of the AMO, the IL is displaced towards the east and the AH towards the west; conversely for a negative AMO phase. Yet, the correspondence with the observational record is unlikely, since the eastward shift of the NAO reported during 1978−1997 applied mainly to the northern center-of-action[16] and coincided with three decades of negative AMO[36].

Until present, a comprehensive explanation for the longitudinal displacements of the NAO pattern remains elusive and the potential role of internal atmospheric variability has yet to be thoroughly investigated. To address this point and revisit previous results, we make use of two 500-year climate simulations performed with EC-EARTH 3.3 (CMIP6 version) and fixed radiative forcing at present-day conditions [year 2000], in atmosphere-only (ATM-ONLY) and coupled ocean-atmosphere (COUPLED) configurations (see Methods). Model data is compared with long-term reanalysis data, namely NOAA 20CR and ERA 20CR. Specifically, we characterize the longitudinal displacements of the IL and examine the processes that could be responsible for them. We show that these eastward/westward shifts are common occurrences and might not require anthropogenic or oceanic forcing but arise from internal atmospheric variability. In particular, our results suggest that these longitudinal displacements are primarily due to zonal changes in variability, rather than climatology, of the regional eddy-driven circulation.

Results

Longitudinal displacements of the Icelandic Low (IL)

To characterize the zonal shifts in the northern lobe of the winter NAO, 30-year running EOFs of detrended SLP anomalies over the North Atlantic-European (NAE) region are computed in both reanalysis and model simulations. For each NAO pattern, the IL location is identified as the anomalous SLP minimum over the northern center-of-action (Fig. 1a). Different running windows (20- and 40-year) have been tested and the results are not sensitive to such parameter (see Methods).

The observed and simulated positions of the IL reveal two preferred regions: the 'western' cluster, with IL locations mainly concentrated south-east of Greenland and west of Iceland; and the 'eastern' cluster, displaying a more dispersed distribution east of Iceland. Interestingly, a general feature is

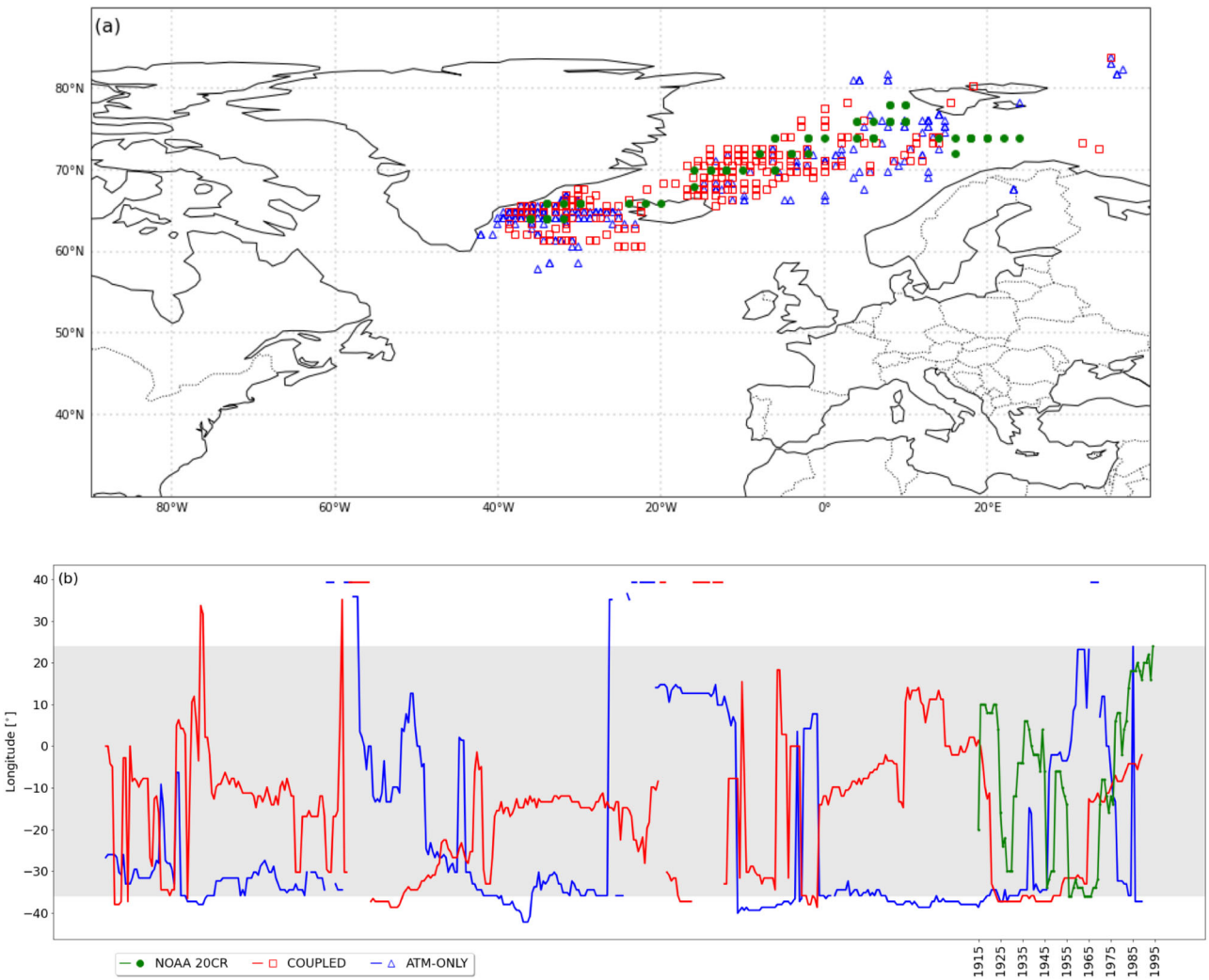

Fig. 1 | Observed and simulated NAO-IL displacements. a Position of the SLP minimum in the northern lobe of the 30-year running first EOF of winter SLP anomalies over the NAE region (20°N-90°N, 90°W-40°E), which corresponds to the spatial variability of the Icelandic Low embedded in the NAO pattern. **b** Longitude of the SLP minimum in those 30-year running NAO patterns in NOAA 20CR (green), COUPLED (red) and ATM-ONLY (blue); IL locations outside the NAE region, i.e., longitudes > 40°E, are not considered. Different datasets are indicated with different colors and symbols, as described in the legend.

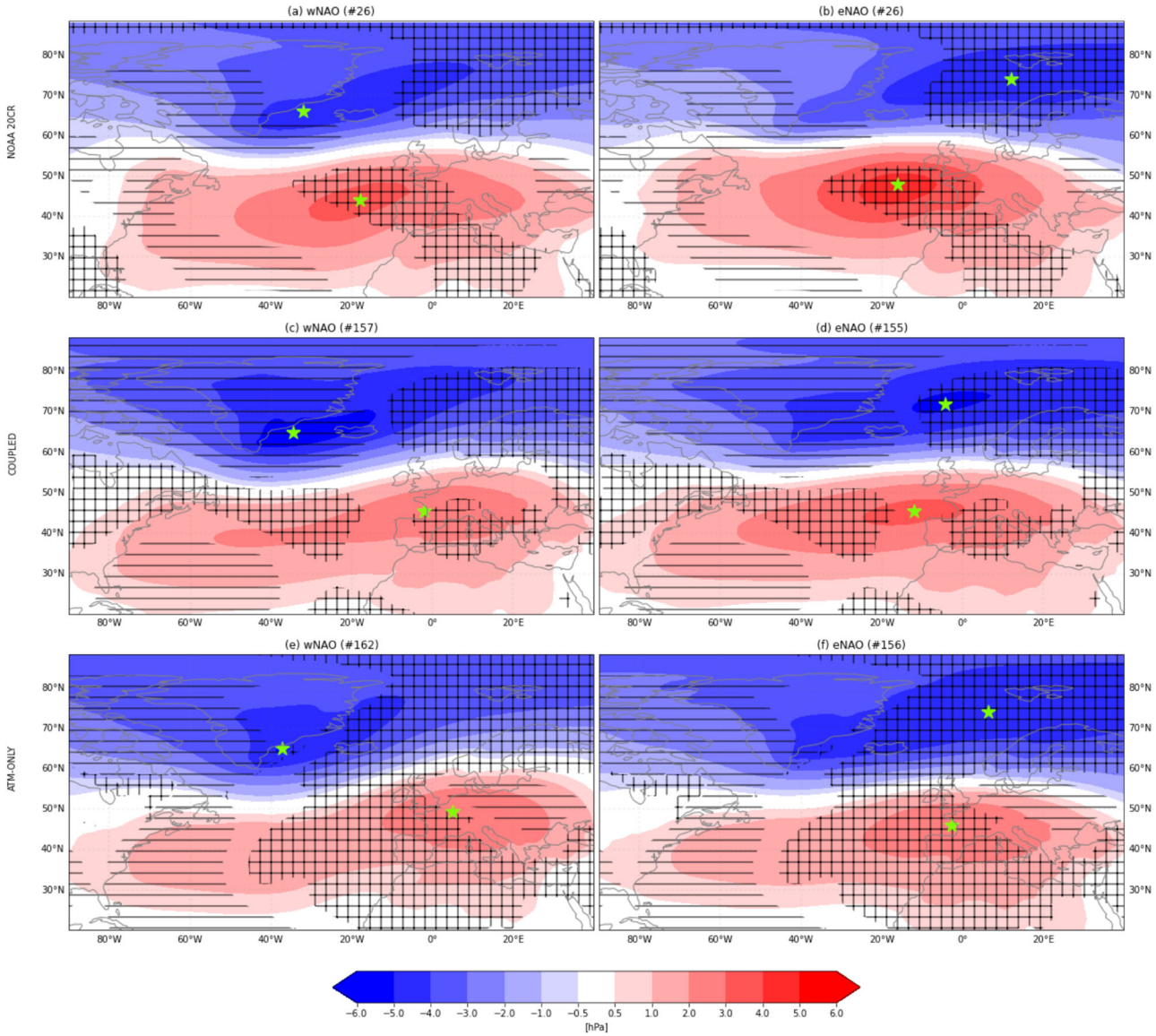

Fig. 2 | Spatial pattern of the NAO-IL displacements. Composite of 30-year running first EOF for western (wNAO; left column) and eastern (eNAO; right column) NAO patterns based on the lower and upper terciles of the Icelandic Low longitude (see text for details): NOAA 20CR (top), COUPLED (middle) and ATM-ONLY (bottom). Hatched areas indicate positive (+) and negative (−) statistically significant differences in SLP variability between eNAO and wNAO composites using a Montecarlo test. Green stars indicate the minimum and maximun SLP anomaly of each composite for the northern (Icelandic Low) and southern (Azores High) lobe, respectively.

that the distinct positions of the IL are distributed over a transversal pathway from the south of Greenland to Svalbard, corresponding to the subpolar low-pressure belt north of the storm-track[37]. Figure 1b shows the time evolution of the IL longitude from 1900 to 2010 in NOAA 20CR (green) and through the 500 years of simulation in COUPLED (red) and ATM-ONLY (blue). We first focus on reanalysis (Fig. 1b; green line), where the IL is located east of Iceland and at around 20°E during the last three decades. As time goes back, the IL moved to the west until reaching values of about 35°W in the 1950s−1960s. This zonal shift is in agreement with Hilmer and Jung[16] who found that the northern lobe of the NAO was displaced eastward during 1978−1997 as compared to 1958−1977. Most subsequent studies on the topic (see Introduction) used the same periods as Hilmer and Jung[16], i.e., considering only the second half of the 20th century. Nevertheless, going further backward in time, when anthropogenic forcing was not that severe, the IL was located again east of Iceland at around 0°E in the 1930s−1940s and 10°E at the beginning of the 20th century, displaying similar values as in the 1970s−1980s.

Linked to the hypothesis of the role played by increasing GHG forcing[28,29] on the eastward shift reported by Hilmer and Jung[16], other studies proposed that the displacement of the IL was associated with the trend towards a positive NAO, and its nonlinear dynamics, that took place during those decades supposedly related to anthropogenic forcing[30,31]. However, later it was shown that such apparent trend in the NAO was not due to global warming but probably to internal variability[34]. Consistent with this latter interpretation, it is worth noting that while the NAO reversed its trend at the beginning of the 21st century and has been oscillating since then, the IL remains in an eastern location since the 1980s (Fig. 1a, b)[38]. Comparing the time evolution of the IL longitude with the NAO index during the entire observational record, it indeed suggests that there is no clear link between both features (Supplementary Fig. 1a); besides, the correlation between these time-series is incoherent in time, which indicates an issue of sampling uncertainty.

In order to overcome the sampling limitation in observational datasets and comprehensively assess low-frequency variability in the NAO

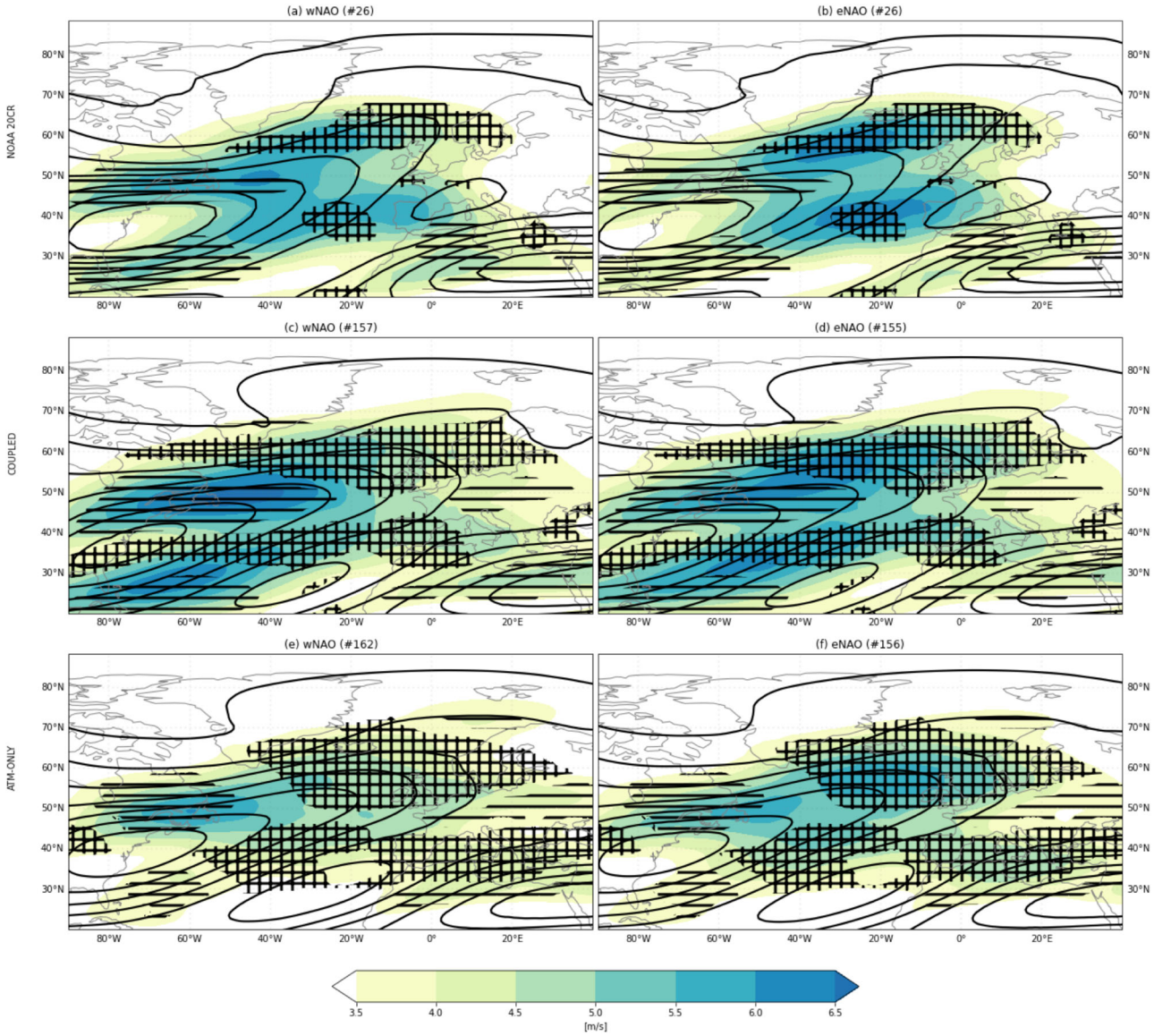

Fig. 3 | Spatial pattern of upper-tropospheric zonal wind in the NAO-IL displacements. Composite of 30-year running climatology (contours, ci: 5 m/s) and standard deviation (shading) of zonal wind at 300 hPa based on the lower (wNAO; left column) and upper (eNAO; right column) terciles of the Icelandic Low longitude (see text for details): NOAA 20CR (top), COUPLED (middle) and ATM-ONLY (bottom). Hatched areas indicate positive (+) and negative (−) statistically significant differences in zonal-wind variability (shading) between eNAO and wNAO composites using a Montecarlo test.

characteristics, 500-year long model experiments have been performed with EC-EARTH (see Methods), which properly simulates the NAO[39,40]. Both experiments have the radiative forcing fixed at present-day conditions, to isolate internally-generated variability from the time-increasing GHG-forced signal. On the other hand, the comparison between COUPLED and ATM-ONLY, the latter with prescribed climatological SSTs, allows addressing the role played by oceanic variability and that internal to the atmosphere.

EC-EARTH realistically simulates the spatial distribution of the IL into western and eastern clusters (Fig. 1a), being both COUPLED and ATM-ONLY almost indistinguishable from reanalysis. The good representation of the NAO pattern and its zonal displacements, particularly of the northern lobe, is confirmed by the time evolution of the IL longitude (Fig. 1b). In both, COUPLED (red) and ATM-ONLY (blue), the IL positions generally fall within the range of the observed IL changes (35°W−25°E; gray shading) and display similar transitions between western and eastern locations.

Lastly, the time evolution of the fraction of variance explained by the NAO has also been investigated (Supplementary Fig. 3), where EC-EARTH, both COUPLED and ATM-ONLY, captures well the range of values in reanalysis (35−55%). The fraction of explained variance and the position of the IL appear to be uncorrelated, implying that the longitudinal displacements of the NAO-IL are independent of the dominance of the NAO pattern in the NAE region.

Western and Eastern NAO composites

The results so far suggest that zonal shifts in the NAO-IL, as the one reported at the end of the 20th century, are recurrent in the climate system and can occur with no need for changes in radiative forcing and/or oceanic variability. We further characterize the preferential locations of the IL by analysing the NAO pattern itself (Fig. 2), computing western (wNAO) and eastern (eNAO) NAO composites based on the lower and upper terciles of the IL longitude, respectively (see Methods).

There is a good agreement between reanalysis (Fig. 2a, b) and model simulations (Fig. 2c−f) in terms of amplitude of SLP anomalies as well as in the position of the northern and southern centers-of-action in the NAO composites. Consistent with Hilmer and Jung[16] and Fig. 1a, the IL position

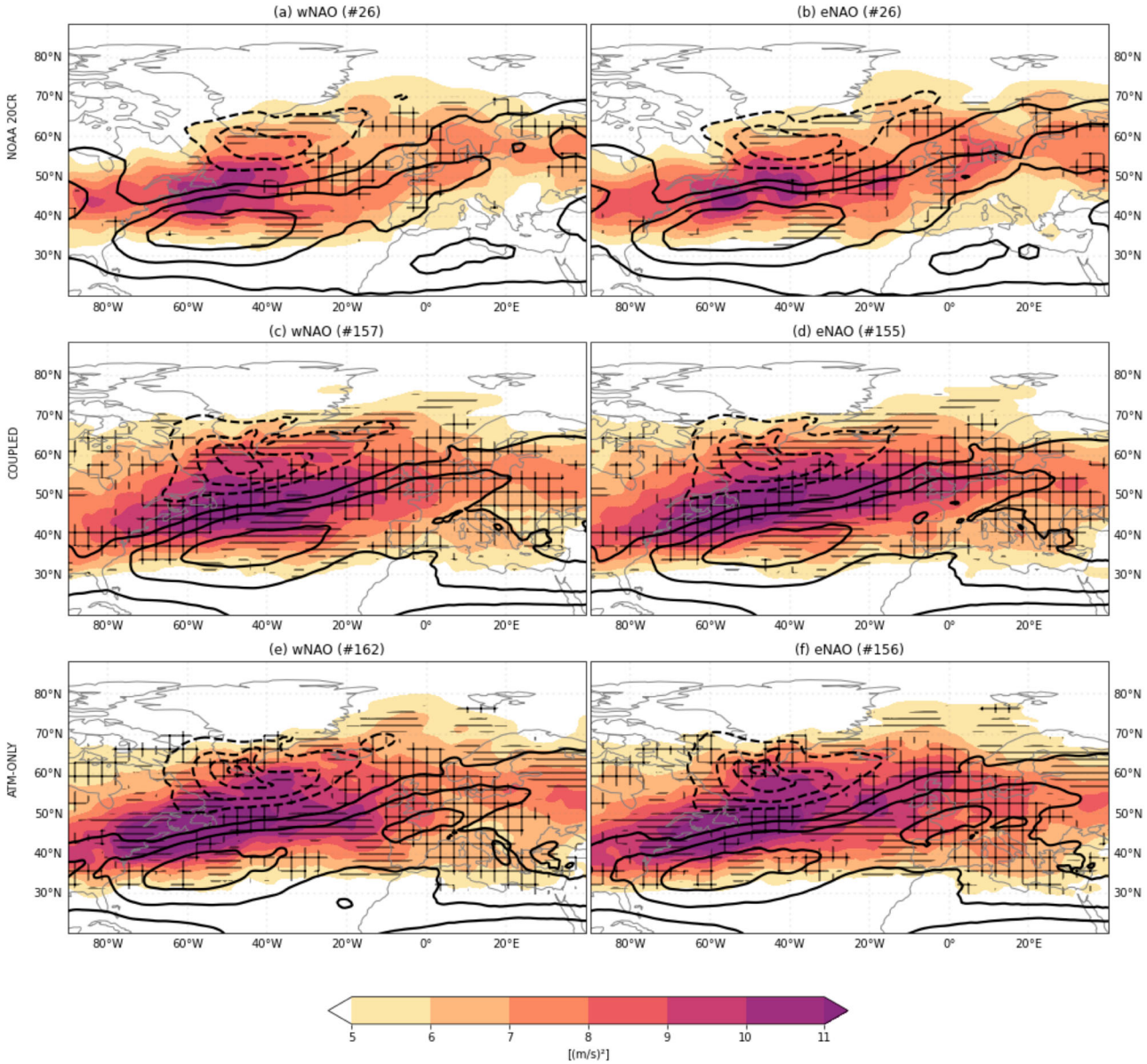

Fig. 4 | Transient-eddy activity in the NAO-IL displacements. Composite of 30-year running climatology (contours, ci: 5 $(m/s)^2$) and standard deviation (shading) of eddy momentum flux, u'v', at 300 hPa based on the lower (wNAO; left column) and upper (eNAO; right column) terciles of the Icelandic Low longitude (see text for details). Hatched areas indicate positive (+) and negative (−) statistically significant differences in eddy momentum flux variability between eNAO and wNAO composites using a Montecarlo test.

in eNAO (Fig. 2-right) displays not only a zonal shift but also a latitudinal shift towards the north compared to wNAO (Fig. 2-left). Noticeably, the AH is almost in the same position for the western and eastern NAO composites, pointing out that longitudinal displacements in the northern lobe do not necessarily go in tandem with those in the southern lobe. Indeed, composites based on the AH longitude show that there is no consistent distinction in the associated NAO pattern with regard to IL locations (Supplementary Fig. 4). Previous studies have suggested that the sensitivity of NAO-IL to zonal displacements is stronger than of NAO-AH[38,41].

In order to explore processes underlying the longitudinal displacements of the IL, several composites of climatology and standard deviation [variability] based on the wNAO/eNAO 30-year periods have been computed. We first analyse SLP. Changes in the composite climatology of SLP between eNAO and wNAO are incoherent among datasets (Supplementary Fig. 5); also, the resulting difference pattern in reanalysis depicts a wNAO signature, inconsistent with the eNAO-wNAO composite, and a positive NAO phase, probably a residual of the apparent trend during the 20th century, pointing at a consequence of sampling uncertainty[42]. In contrast, changes in the composite standard deviation of SLP show a coherent and significant pattern in reanalysis and model simulations, displaying an increase in SLP variability over the eastern part of the NAE region, particularly east of Iceland, and a decrease over the western part (Supplementary Fig. 6; hatching in Fig. 2). Note also changes in amplitude and tilting over the eastern mid-latitudes, although they do not translate into changes of the AH position, as discussed above. Hence, these results indicate that zonal shifts of the IL project on changes in SLP variability and not in SLP climatology, which is consistent with the nature of the NAO being a mode of atmospheric variability.

NAO dynamics

The NAO can be considered as the integrator or main manifestation of latitudinal wobbling in the North Atlantic eddy-driven jet[8,43]. We now

investigate changes in upper-tropospheric zonal wind [300 hPa; U300] according to wNAO/eNAO composites (Fig. 3).

EC-EARTH correctly simulates the climatology of the jet in terms of location and magnitude (Fig. 3, contours), displaying a maximum over the East Coast of North America that elongates north-eastward across the North Atlantic Ocean. Changes in the composite climatology of U300 were again incoherent among datasets (not shown). Variability of the jet is also well captured by the model (Fig. 3, shading), yielding the observed dipole of standard deviation at both sides of the jet; although in ATM-ONLY the dipole is less evident, with a stronger (weaker) signal to the north (south), probably due to the experimental setup lacking air-sea interaction and using observed SSTs, not simulated SSTs (see Methods). Even so, changes in the composite standard deviation of U300 between eNAO and wNAO are remarkably consistent among datasets and statistically significant, showing an increase of variability in the exit region of the jet and a decrease in the core region. That these difference patterns project on a zonal shift of the variability dipole, which is tightly related to meridional variations of the eddy-driven jet and storm-track[1,43], indicate that the longitudinal displacements of the NAO-IL are associated with NAO dynamics at interannual-to-decadal timescales not at multi-decadal[38,41,44].

The connection with changes in the stratospheric circulation has also been analysed (Supplementary Fig. 8). There appears to be no clear link between the wNAO/eNAO composites and troposphere-stratosphere coupling in reanalysis, while model simulations show no coherent changes, with COUPLED depicting a particularly weak signal. NOAA 20CR and ATM-ONLY display a decrease in variability of the polar vortex [10 hPa, 60°N[45]] for eNAO as compared to wNAO, which is inconsistent with the increase in variability of the zonal wind at 300 hPa (Fig. 3). These results suggest that zonal shifts of the IL rely mainly on processes of tropospheric circulation.

Finally, we evaluate composites of transient-eddy momentum flux (u'v') in the upper troposphere[6] (see Methods), since it is a key eddy diagnostic to characterize NAO dynamics, being fundamental for acceleration/deceleration as well as meridional migrations of the jet[46–48]. Figure 4 shows the wNAO/eNAO composites of u'v' climatology (contours) and standard deviation (shading), where both model experiments properly simulate the observed signals. In particular, the climatological pattern displays positive values at middle latitudes (northward transport of westerly momentum) and negative values at subpolar latitudes (southward transport of westerly momentum), whose convergence leads to the North Atlantic eddy-driven jet[3,48] (Fig. 3, contours). The variability pattern is maximum along this line of convergence, which is interpreted as variations in the eddy forcing of the mean flow. Again, changes in the composite climatology were incoherent among datasets (not shown), in agreement with the changes reported above in SLP and U300 climatology. On the contrary, changes in the composite standard deviation of u'v' between eNAO and wNAO are consistent among datasets and statistically significant, showing an increase of variability over the exit region of the jet that tilts north-eastward. Thereby, the longitudinal displacements of the NAO-IL appear to be associated with NAO dynamics at interannual-decadal timescales and mediated by transient-eddy activity.

Discussion

In the wake of Hilmer and Jung's[16] seminal work evidencing an eastward shift of the winter NAO-IL during the second half of the 20th century, several studies interpreted this shift as a (potential) new spatial regime for the winter NAO, likely related to a concomitant trend towards a positive NAO phase attributable to anthropogenic forcing and related ocean warming[28,29,31]. However, our results, using long-term reanalysis data spanning the entire 20th century to 2010 (NOAA 20CR and ERA 20CR), reveal that the reported eastward shift of the Icelandic Low is not a one-time event. Indeed, they show that such NAO-IL longitudinal displacements are recurrent and can be categorized into two distinct clusters: 'western' and 'eastern' NAO patterns, corresponding to IL locations west and east of Iceland, respectively. Even so, the observational record might be limited as to properly assess some NAO characteristics[42]; hence, we have also used long model simulations (500 years) with fixed radiative forcing at present-day conditions, namely coupled and atmosphere-only. With this experimental setup and the consistency across datasets, our findings suggest that these recurrent 'western' and 'eastern' NAO clusters are primarily determined by internal atmospheric variability.

The NAO-IL longitudinal displacements are not casual but causal, as they take place along the North Atlantic subpolar low-pressure belt. Likewise, the variability of the North Atlantic eddy-driven jet and storm-track manifest as latitudinal migrations in both NAO clusters but with a distinctive zonal shift, which implies a central role played by intrinsic NAO-related atmospheric dynamics at interannual-to-decadal timescales[44]. Diagnostics for the reported eastward shift[16] such as wave breaking[32], blocking[33], non-linearity[30,31], and strength[49] and meridional excursion of the westerly wind[38,41] are consistent with the positive trend of the NAO index at the time, but cannot easily explain the 'western' and 'eastern' clusters because they are based on the NAO phase and not on the NAO spatial pattern itself (including both NAO+/NAO–). Our results are in agreement with previous studies showing that zonal changes of the mean flow (SLP) in terms of standard deviation, not climatology, are reflected into zonal changes of the NAO pattern, particularly the northern lobe[17,50]. They are also aligned with those pointing at a key role played by internal atmospheric variability via zonal shifts of transient-eddy activity[38,41].

While the ultimate mechanism of the recurrent NAO-IL longitudinal displacements is not clear, i.e., why systematically west or east of Iceland, and an additional effect of anthropogenic forcing cannot be discarded[28], the environmental impacts of NAO spatial variations in future climate can be very relevant. According to our results, internal variability could affect Euro-Atlantic near-term climate predictions/projections not only associated with the NAO polarity[42] but also with the NAO-Icelandic Low cluster.

Methods

Reanalysis and model data

The NOAA-CIRES 20th Century Reanalysis version 2c (NOAA 20CR[51]) has been used on the original 2° × 2° longitude-latitude resolution; T62 Gaussian grid [192 × 94]. The temporal coverage spans from 1900 to 2010, to match with the ECMWF 20th Century Reanalysis (ERA 20CR[52]; T159 [320 × 160]) and, thus, assess observational uncertainty. The results using both reanalyses are almost identical; so that, we only report those from NOAA 20CR, although they are collectively referred to as 'reanalysis' in the text, unless otherwise specified. We use monthly data for sea level pressure and zonal wind at 300 hPa, and daily data for zonal and meridional wind to compute transient-eddy diagnostics (see below).

Two 500-year climate simulations, after spin-up, performed with EC-EARTH 3.3 (CMIP6 version[40]) at a horizontal resolution of 0.7° × 0. 7° longitude-latitude [T255; 512 × 256] and 91 vertical levels [top 0.01 hPa] have been performed and analysed. Coupled ocean-atmosphere (COUPLED) and atmosphere-only (ATM-ONLY) configurations have been used. To partially separate results from the model framework and for ease of comparison, observational SSTs were employed in the latter, which is based on the setup of SPARC-QBOi's "Experiment 2"[53]: time-slice simulation with prescribed, repeated seasonal cycle for SST and sea ice concentration (SIC) whose climatology is computed over 1988−2007, and fixed radiative forcing, aerosols and chemical constituents (including ozone) at year 2000, which is well removed from any explosive volcanic eruption and is representative of present-day conditions. Hence, there is no interannual variability or secular change in the applied forcings. Both boundary conditions and radiative forcing/atmospheric composition were taken from the CMIP6 input dataset. The model performance in 100 years of ATM-ONLY is reported in Palmeiro et al.[54]. On the other hand, the coupled simulation started from a historical run and kept radiative forcing/atmospheric composition fixed as in ATM-ONLY. The model performance in 250 years of COUPLED is reported in Volpi et al.[55].

NAO pattern and index

Empirical orthogonal function (EOF[56]) analysis is used to define the NAO index as the leading principal component (PC1), namely

standardized time series, corresponding to the leading mode (EOF1) of winter SLP anomalies in the North Atlantic-European region (NAE[1]: 20°N-90°N, 90°W-40°E). We compute 30-year running EOFs from 1900 to 2010 in reanalysis and over the 500 years of simulation in COUPLED and ATM-ONLY. Note that different running windows (20-, 30- and 40-year) have been tested and the results are very similar. A 30-year period was chosen for reporting inspired by the World Meteorological Organization (WMO) standard for climatological normals. Since the main focus of this study is on the longitudinal displacements of the northern lobe of the NAO, we set all NAO patterns (EOF1s) to be in its positive phase. All anomalies were quadratically detrended before analysis.

Western and Eastern NAO composites

The Icelandic Low (IL) location is identified as the anomalous SLP minimum over the northern center-of-action in each running EOF. Composites of western and eastern NAO patterns are based on the lower and upper terciles, respectively, of the probability density function of the IL longitude (Fig. 1); namely, considering longitudes further west (east) than the lower (upper) tercile for wNAO (eNAO). Note that in ATM-ONLY, this criterion was modified for the western composite (wNAO) by considering also longitudes equal to the lower tercile, in order to retain more sampling, since there were several IL locations at that value. To assess statistical significance in the difference of composite climatology and standard deviation between eNAO and wNAO, we perform a Monte Carlo test based on 100 iterations. It consists in generating a probability density function to compute the significance level (p-value) which corresponds to the number of randomized values that exceed the actual value being tested[57]. To do so, we randomly generate wNAO/eNAO composites by creating 30-year periods by shuffling winters over the whole period (1900−2010 in reanalysis; 500 years in model simulations) with replacement.

Transient-eddy activity

Transient-eddy diagnostics are computed using daily data at 300 hPa. Zonal (u) and meridional (v) wind are employed to analyse eddy-mean flow interaction through the eddy momentum flux [u'v'] and eddy kinetic energy [EKE=0.5(u'u'+v'v')], where the time-mean covariances have been computed from filtered daily data using a 24-h difference filter[37,58]. Results for eddy momentum flux and EKE are similar, so only the former is reported here. Accidentally, daily data from the EC-EARTH simulations were only available at 500 hPa and 100 hPa; so that, we compute 300-hPa u'v' as the average of eddy momentum flux between both pressure levels. We have tested this approach with reanalysis data and the same spatial patterns were obtained, albeit with slightly different magnitude. Likewise, computing first the averaged wind components (u', v') and then the eddy covariance provides similar values.

Data availability

Reanalysis data used in this study can be retrieved from publicly available repositories:

- NOAA-CIRES 20th Century Reanalysis V2c[51]: https://psl.noaa.gov/data/gridded/data.20thC_ReanV2c.html
- ECMWF Reanalysis of the 20th Century (ERA-20C)[52]: https://www.ecmwf.int/en/forecasts/dataset/ecmwf-reanalysis-20th-century

EC-EARTH simulations can be provided upon reasonable request.

Code availability

The source codes used in this study are available from the corresponding author upon request.

Received: 13 June 2024; Accepted: 12 November 2024;
Published online: 30 November 2024

References

1. Hurrell, J. W., Kushnir, Y., Ottersen, G. & Visbeck, M. An overview of the North Atlantic Oscillation. *Geophys. Monogr. Am. Geophys. Union* **134**, 1–36 (2003).
2. Hurrell, J. W. & Deser, C. North Atlantic climate variability: the role of the North Atlantic Oscillation. *J. Mar. Syst.* **79**, 231–244 (2010).
3. Vallis, G. K. & Gerber, E. P. Local and hemispheric dynamics of the North Atlantic Oscillation, annular patterns and the zonal index. *Dyn. Atmos. Oceans* **44**, 184–212 (2008).
4. Limpasuvan, V. & Hartmann, D. L. Wave-maintained annular modes of climate variability. *J. Clim.* **13**, 4414–4429 (2000).
5. Rivière, G. & Orlanski, I. Characteristics of the Atlantic storm-track eddy activity and its relation with the North Atlantic Oscillation. *J. Atmos. Sci.* **64**, 241–266 (2007).
6. Feldstein, S. B. The dynamics of NAO teleconnection pattern growth and decay. *Q. J. R. Meteorol. Soc.* **129**, 901–924 (2003).
7. Marshall, J. et al. North Atlantic climate variability: phenomena, impacts and mechanisms. *Int. J. Climatol. J. R. Meteorol. Soc.* **21**, 1863–1898 (2001).
8. Woollings, T., Hannachi, A. & Hoskins, B. Variability of the North Atlantic eddy-driven jet stream. *Q. J. R. Meteorol. Soc.* **136**, 856–868 (2010).
9. Martineau, P., Nakamura, H., Kosaka, Y., Taguchi, B. & Mori, M. Modulations of North American and European weather variability and extremes by interdecadal variability of the atmospheric circulation over the North Atlantic sector. *J. Clim.* **33**, 8125–8146 (2020).
10. Luo, D., Yao, Y. & Feldstein, S. B. Regime transition of the North Atlantic Oscillation and the extreme cold event over Europe in January–February 2012. *Monthly Weather Rev.* **142**, 4735–4757 (2014).
11. Diao, Y., Xie, S.-P. & Luo, D. Asymmetry of winter European surface air temperature extremes and the North Atlantic Oscillation. *J. Clim.* **28**, 517–530 (2015).
12. Beniston, M. & Jungo, P. Shifts in the distributions of pressure, temperature and moisture and changes in the typical weather patterns in the alpine region in response to the behavior of the North Atlantic Oscillation. *Theor. Appl. Climatol.* **71**, 29–42 (2002).
13. López-Moreno, J. et al. Effects of the North Atlantic Oscillation (NAO) on combined temperature and precipitation winter modes in the Mediterranean mountains: Observed relationships and projections for the 21st century. *Glob. Planet. Change* **77**, 62–76 (2011).
14. Guo, Y. et al. Quantifying excess deaths related to heatwaves under climate change scenarios: A multicountry time series modelling study. *PLoS Med.* **15**, e1002629 (2018).
15. Roson, R., Calzadilla, A. & Pauli, F. Climate change and extreme events: an assessment of economic implications. FEEM Working Paper No 44, University Ca' Foscari of Venice, Dept. of Economics Research Paper Series No 18 https://ssrn.com/abstract=893035/06, https://ssrn.com/abstract=893035 or https://doi.org/10.2139/ssrn.893035 (2006).
16. Hilmer, M. & Jung, T. Evidence for a recent change in the link between the North Atlantic Oscillation and Arctic sea ice export. *Geophys. Res. Lett.* **27**, 989–992 (2000).
17. Jung, T. et al. Characteristics of the recent eastward shift of interannual NAO variability. *J. Clim.* **16**, 3371–3382 (2003).
18. Cassou, C., Terray, L., Hurrell, J. W. & Deser, C. North Atlantic winter climate regimes: spatial asymmetry, stationarity with time, and oceanic forcing. *J. Clim.* **17**, 1055–1068 (2004).
19. Zhang, X., Jin, L., Chen, C., Guan, D. & Li, M. Interannual and interdecadal variations in the North Atlantic Oscillation spatial shift. *Chin. Sci. Bull.* **56**, 2621–2627 (2011).
20. Wang, Y.-H., Magnusdottir, G., Stern, H., Tian, X. & Yu, Y. Decadal variability of the NAO: Introducing an augmented NAO index. *Geophys. Res. Lett.* **39**, (2012). https://doi.org/10.1029/2012GL053413.

21. Pinto, J. G. & Raible, C. C. Past and recent changes in the North Atlantic Oscillation. *Wiley Interdiscip. Rev. Clim. Change* **3**, 79–90 (2012).
22. Lu, J. & Greatbatch, R. J. The changing relationship between the NAO and northern hemisphere climate variability. *Geophys. Res. Lett.* **29**, 52–1 (2002).
23. Polyakova, E. I., Journel, A. G., Polyakov, I. V. & Bhatt, U. S. Changing relationship between the North Atlantic Oscillation and key North Atlantic climate parameters. *Geophys. Res. Lett.* **33**, (2006). https://doi.org/10.1029/2005GL024573.
24. Lehmann, A., Getzlaff, K. & Harlaß, J. Detailed assessment of climate variability in the Baltic Sea area for the period 1958 to 2009. *Clim. Res.* **46**, 185–196 (2011).
25. Vicente-Serrano, S. M. & López-Moreno, J. I. Nonstationary influence of the North Atlantic Oscillation on European precipitation. *J. Geophys. Res. Atmos.* **113**, (2008). https://doi.org/10.1029/2008JD010382.
26. Beranová, R. & Huth, R. Time variations of the effects of circulation variability modes on European temperature and precipitation in winter. *Int. J. Climatol. J. R. Meteorol. Soc.* **28**, 139–158 (2008).
27. Filippi, L., Palazzi, E., von Hardenberg, J. & Provenzale, A. Multidecadal variations in the relationship between the NAO and winter precipitation in the Hindu Kush–Karakoram. *J. Clim.* **27**, 7890–7902 (2014).
28. Ulbrich, U. & Christoph, M. A shift of the NAO and increasing storm track activity over Europe due to anthropogenic greenhouse gas forcing. *Clim. Dyn.* **15**, 551–559 (1999).
29. Dong, B., Sutton, R. T. & Woollings, T. Changes of interannual NAO variability in response to greenhouse gases forcing. *Clim. Dyn.* **37**, 1621–1641 (2011).
30. Peterson, K. A. et al. Hindcasting the NAO using diabatic forcing of a simple AGCM. *Geophys. Res. Lett.* **29**, 50–1 (2002).
31. Peterson, K. A., Lu, J. & Greatbatch, R. J. Evidence of nonlinear dynamics in the eastward shift of the NAO. *Geophys. Res. Lett.* **30**, (2003). https://doi.org/10.1029/2002GL015585.
32. Wang, Y.-H. & Magnusdottir, G. The shift of the northern node of the NAO and cyclonic Rossby wave breaking. *J. Clim.* **25**, 7973–7982 (2012).
33. Davini, P., Cagnazzo, C., Neale, R. & Tribbia, J. Coupling between Greenland blocking and the North Atlantic Oscillation pattern. *Geophys. Res. Lett.* **39**, (2012). https://doi.org/10.1029/2012GL052315.
34. Blackport, R. & Fyfe, J. C. Climate models fail to capture strengthening wintertime Europe Atlantic jet and impacts on Europe. *Sci. Adv.* **8**, eabn3112 (2022).
35. Börgel, F., Frauen, C., Neumann, T. & Meier, H. M. The Atlantic Multidecadal Oscillation controls the impact of the North Atlantic Oscillation on north European climate. *Environ. Res. Lett.* **15**, 104025 (2020).
36. Deser, C., Alexander, M. A., Xie, S.-P. & Phillips, A. S. Sea surface temperature variability: patterns and mechanisms. *Annu. Rev. Mar. Sci.* **2**, 115–143 (2010).
37. Chang, E. K., Lee, S. & Swanson, K. L. Storm track dynamics. *J. Clim.* **15**, 2163–2183 (2002).
38. Luo, D., Zhu, Z., Ren, R., Zhong, L. & Wang, C. Spatial pattern and zonal shift of the North Atlantic Oscillation. Part I: a dynamical interpretation. *J. Atmos. Sci.* **67**, 2805–2826 (2010).
39. Haarsma, R. et al. HighResMIP versions of EC-Earth: EC-Earth3P and EC-Earth3P-HR. Description, model performance, data handling and validation. *Geosci. Model Dev. Discuss.* **2020**, 1–37 (2020).
40. Döscher, R. et al. The EC-Earth3 Earth system model for the Climate Model Intercomparison Project 6. *Geosci. Model Dev. Discuss.* **2021**, 1–90 (2021).
41. Luo, D., Zhong, L., Ren, R. & Wang, C. Spatial pattern and zonal shift of the North Atlantic Oscillation. Part II: Numerical experiments. *J. Atmos. Sci.* **67**, 2827–2853 (2010).
42. Deser, C., Hurrell, J. W. & Phillips, A. S. The role of the North Atlantic Oscillation in European climate projections. *Clim. Dyn.* **49**, 3141–3157 (2017).
43. Thompson, D. W., Lee, S. & Baldwin, M. P. Atmospheric processes governing the Northern Hemisphere Annular Mode/North Atlantic Oscillation. *North Atl. Oscillation: Clim. Significance Environ. impact* **134**, 81–112 (2003).
44. Woollings, T. et al. Contrasting interannual and multidecadal NAO variability. *Clim. Dyn.* **45**, 539–556 (2015).
45. Charlton, A. J. & Polvani, L. M. A new look at stratospheric sudden warmings. Part I: Climatology and modeling benchmarks. *J. Clim.* **20**, 449–469 (2007).
46. Hoskins, B. J., James, I. N. & White, G. H. The shape, propagation and mean-flow interaction of large-scale weather systems. *J. Atmos. Sci.* **40**, 1595–1612 (1983).
47. Thorncroft, C., Hoskins, B. & McIntyre, M. Two paradigms of baroclinic-wave life-cycle behaviour. *Q. J. R. Meteorol. Soc.* **119**, 17–55 (1993).
48. Vallis, G. K. *Atmospheric and oceanic fluid dynamics* (Cambridge University Press, 2017).
49. Luo, D. & Gong, T. A possible mechanism for the eastward shift of interannual NAO action centers in last three decades. *Geophys. Res. Lett.* **33**, (2006). https://doi.org/10.1029/2006GL027860.
50. Haarsma, R. J. et al. Sensitivity of winter North Atlantic-European climate to resolved atmosphere and ocean dynamics. *Sci. Rep.* **9**, 13358 (2019).
51. Compo, G. P. et al. The twentieth century reanalysis project. *Q. J. R. Meteorol. Soc.* **137**, 1–28 (2011).
52. Poli, P. et al. ERA-20C: an atmospheric reanalysis of the twentieth century. *J. Clim.* **29**, 4083–4097 (2016).
53. Butchart, N. et al. Overview of experiment design and comparison of models participating in phase 1 of the SPARC Quasi-Biennial Oscillation initiative (QBOi). *Geosci. Model Dev.* **11**, 1009–1032 (2018).
54. Palmeiro, F. M. et al. Boreal winter stratospheric climatology in EC-EARTH: CMIP6 version. *Clim. Dyn.* **60**, 883–898 (2023).
55. Volpi, D., García-Serrano, J., Palmeiro, F. M., Gil-Reyes, L. & Haarsma, R. J. Tropical Atlantic variability in EC-EARTH: impact of the radiative forcing. *Clim. Dyn.* 1–15 (2024).
56. von Storch, H. Spatial patterns: EOFs and CCA. In von Storch, H., Navarra, A. (eds) Analysis of Climate Variability: Applications of Statistical Techniques Proceedings of an Autumn School Organized by the Commission of the European Community on Elba from October 30 to November 6, 231–263 (Springer, Berlin, Heidelberg, 1999).
57. García-Serrano, J., Frankignoul, C., Gastineau, G. & de La Cámara, A. On the predictability of the winter Euro-Atlantic climate: Lagged influence of autumn Arctic sea ice. *J. Clim.* **28**, 5195–5216 (2015).
58. Wallace, J. M., Lim, G.-H. & Blackmon, M. L. Relationship between cyclone tracks, anticyclone tracks and baroclinic waveguides. *J. Atmos. Sci.* **45**, 439–462 (1988).

Acknowledgements

MS-O was supported by a 'Margarita Salas' fellowship from the Spanish Ministry of Universities. This study received funding from the Spanish DYNCAST project (CNS2022-135312). Open Access funding provided by 'Ajuts de la Universitat de Barcelona 2024' and the Group of Meteorology (METEO-UB; 2021-SGR-01074). Red Española de Supercomputación is acknowledged for awarding computing resources (RES projects AECT-2019-2-0019 and AECT-2020-3-0009). Technical support at Barcelona Supercomputing Center is sincerely acknowledged. The authors are thankful to three anonymous reviewers for their comments.

Author contributions

M.S.-O. and J.G.-S. conceived the study. J.G.-S. ran the simulations. M.S.-O. conducted the analysis and prepared the figures. Both authors wrote the manuscript.

Competing interests

The authors declare no competing interests.

Additional information

Supplementary information The online version contains supplementary material available at https://doi.org/10.1038/s41612-024-00842-8.

Correspondence and requests for materials should be addressed to María Santolaria-Otín.